

# **CHAPTER 3**

## **Methodology**

## CHAPTER 3

### 3.1 Epitome of methodology

In the present chapter, methodology adopted for present work has been presented into subdivisions including synthesis of catalyst, characterization of catalyst, transesterification reaction, optimization and characterization of biodiesel. At first, catalyst was synthesized by solid state and co-precipitation methods respectively. Then, characterization of catalyst was investigated by various techniques. The methods for determination of physicochemical properties of the catalyst have been discussed. Subsequently, catalyst activity was assessed by transesterification of feedstocks namely waste vegetable oil and Karanja oil with methanol to produce biodiesel. Reusability of catalyst was assessed to study its durability. The conversion of fatty acid methyl ester (biodiesel) was calculated by using  $^1\text{H}$  NMR. Physicochemical property of biodiesel was estimated as per ASTM standards.

### 3.2 Synthesis of catalyst

#### 3.2.1 Synthesis via solid state method

In solid state method, appropriate amounts of solid phase materials mixed together in a ball mill due to their hardness as well as smooth and non-porous surface. In order to assist the homogenization of the mixture in addition to grinding, adequate quantity of some volatile organic liquid, acetone was added in mixture through grinding. After complete vaporization of acetone, fine powder was obtained. This was calcined to obtain desired product at specific temperature.

### 3.2.2 Synthesis by co-precipitation method

Co-precipitation is carried out by a precipitate of material usually soluble under the applied conditions. Advantage of co-precipitation method involves the ease of handling and its simplicity at specific pH conditions [Xia et al., 2011]. This method also shows some detriments such as final product contamination through metal base and inhomogeneous distribution of composition [Jeffrey and Brinker, 1990]. Co-precipitation can be improved by introducing other chemical species to dispense superior complexation with avoiding precipitation of detrimental material as a substitute of simple addition of salt metal solutions to the strong basic solution [Silva, 2004].

### 3.3 Characterization of catalyst

Physicochemical properties of synthesized catalyst were studied by several characterization techniques and were explained as follows:

#### 3.3.1 Thermogravimetric analysis (TGA)

Thermogravimetric analysis (TGA) is an analytical method of thermal analysis used to measure the mass transformation as a function of temperature (at constant heating rate) or time (at constant temperature and mass loss). Usually, TGA is used to demonstrate characteristics of materials that reveal mass gain or loss due to loss of volatile matter (moisture), oxidation or decomposition. The measurement is carried out in presence of air or in inert atmosphere (helium or argon) and mass change is recorded as a function of temperature rise. As sample is heated, it can lose weight by drying or release of various gases. The data can be plotted as weight percent (%) or time vs temperature (°C) in form of thermogram which shows the thermal stability of sample [Gabbott, 2008].

TGA was performed on Perkin Elmer Pyris 1 model in oxidative atmosphere of mixture of air and inert gas. Maximum temperature was chosen for stability of sample implies the completion of all chemical reactions. Sample was placed on sample holder made up of alumina supported on microbalance. The sample starts heating with the rate of 20 °C/min starting from 40 °C to 1000 °C temperature range. The balance sends the signal of weight, sample temperature as well as elapsed time to the system. Resulting curve obtained was steeper with close onset temperature.

### 3.3.2 Powder X-ray diffraction (XRD)

In order to apprehend the crystalline structure of sample during thermal decomposition, X-ray diffraction (XRD) analysis of the catalyst was performed. XRD has been used to study the exact situation of ions present in ionic crystal lattice within molecule by giving exact bond angle and bond length values of any molecule [Duckett and Gilbert, 2000]. Chemical bonds and non-covalent interactions can be better understood by X-ray crystallography. X-ray diffraction betides when monochromatic beam of X-ray interacts with material and scattered in different direction without absorption of any ray. XRD is useful to identify size and shape of unit cell as well as for atomic number and position of atoms occurred in the cell. Sample is considered to be X-ray pure if the entire lines were indexed.

X-ray diffraction (XRD) was performed on Rigaku MiniFlex 600 by using SC-70 detector and continuous scan mode as well as X-ray of 40 kV, 15 mA. Sample was pulverised into powder form and placed on sample holder, afterwards scanned by using CuK $\alpha$  radiation. Data were composed over the 2 $\theta$  range of 5° – 80° with the scanning rate of 5 degree/min. Diffraction patterns observed in XRD were assimilated according to the

Joint Committee on Powder Diffraction Standards (JCPDS).

### **3.3.3 Attenuated total reflectance Fourier transform infrared spectroscopy (ATR-FTIR)**

Functional group and type of bond can be easily identified by Fourier-transform infrared (FT-IR) spectroscopy. The X-ray diffraction (XRD) technique is not more effective in estimating the appearance of non-crystalline phases present in the sample when compound acquaint on surface of the sample. This technique is more sensitive for assimilation of phases. This technique can be employed to quantify the components of unknown organic or inorganic sample. Absorption fingerprint region in FT-IR spectra of sample resembles to vibration frequency between atomic bonds which is unique for each sample [Griffiths and Haseth, 2007]. Inorganic compound shows simple spectra, whereas organic compound displays detailed spectra. Unknown samples can be recognized by comparing their spectrum with library of known sample.

The FTIR spectra of catalyst were collected on ALPHA BRUKER Eco-ATR furnished with ZnSe ATR crystal in the range of 500-4000  $\text{cm}^{-1}$  with 25 scans.

### **3.3.4 Brunauer-Emmett-Teller (BET) surface area and BJH analysis**

Physical adsorption of gaseous molecules on the solid surface of catalyst due to weak van der Waals forces between adsorbate (gas molecules) and adsorbent surface area (catalyst) is measured by using Brunauer-Emmett-Teller (BET) surface area analysis [Brunauer et al., 1938]. The concept of BET is perpetuation of the Langmuir isotherm that is monolayer to multilayer molecular adsorption with assumptions: infinite layer of physical adsorption of gas molecules on surface, each adsorption layer has no interaction and Langmuir theory can be employed to respective layer. The technique includes

external area and pore area estimates to define the total specific surface area in  $\text{m}^2/\text{g}$  shows significant information for the effect of surface porosity. With this, BJH analysis is used to study the pore area and pore volume by using adsorption and desorption techniques. Total pore volume of catalyst is obtained from volume of vapour adsorbed at temperature near to unity. Whereas, the average pore size is assessed from pore volume.

Surface area of synthesized catalyst were analysed on Micromeritics TriStar -3000 surface area analyser by using standard Brunauer-Emmett-Teller (BET) method. Sample was degassed at  $200\text{ }^\circ\text{C}$  for 3 h under a nitrogen atmosphere to eradicate the physisorbed moisture of the catalyst. Nitrogen adsorption-desorption was carried out at  $-195.73^\circ\text{C}$  after 10 seconds of equilibrium interval and automatic degassing. It is essential to eradicate the vapours and gases that physically adsorbed on surface of catalyst after synthesis. If sample is not degassed, some area will be covered by earlier adsorbed vapour of gaseous molecules which decreases specific surface area of catalyst. To maintain nature as well as property of surface, degassing time and temperature must keep as low as possible.

### **3.3.5 Scanning electron microscopy (SEM) and energy dispersive X-ray spectroscopy (EDS)**

Morphologies of the synthesized catalytic crystals were explored by using scanning electron microscopy (SEM). SEM has many advantages such as high depth field, uses electromagnet due to which facilitates to focus more specimens at a time as well as higher magnification and resolution. Sample was coated with gold in vacuum conditions by sputter coater. In sputter coater, electron is detached from argon and becomes positively charged due to appliance of electric field. This positively charged

argon attracts negatively charged gold foil and hits the surface of gold foil and due to which gold atoms drop and get coated on the sample surface.

The variations in the composition of the bond interface were studied by using energy dispersive X-ray spectroscopy (EDS). The EDS is attached to the scanning electron microscope (SEM) and the two techniques are frequently used together. The X-rays have energies that are characteristic of the elements present in the sample. EDS is predominantly good for elemental alignment concerned to topographical structures. Unknown samples can be recognized and quantitative analysis can be executed with the help of EDS.

Scanning electron microscopy (SEM) combined with energy dispersive X-ray spectroscopy (EDS) was recorded on ZEISS EVO 18 SEM coating of quorum Q150R ES (Model 51-ADD0048).

### 3.3.6 Particle size analysis

The diameter of particle was measured with the particle size analyser based on the principle of dynamic light scattering (DLS) method. In DLS photon correlation spectroscopy (PCS) measures the intensity size distribution (weighted) and represented in the form of histogram. Magnitude of every peak is proportional to percent of overall scattered intensity through particles. This instrument calculates intensity distributions and can convert them to volume or number distributions. A volume distribution (equivalent to weight distributions) will provide the relative volume of particles for each size present in sample. Results obtained from intensity were dependent on scattering angle whereas in case of volume it is independent. Number distribution can be calculated by volume percentage result divided by cubed diameter of particles. The corresponding % in each



beam can be achieved from table of size distribution.  $\ln(G2(t)-1)$  plot displays the natural logarithmic graph designates the presence of any noise in the signal.

Particle size was analysed on Delsa™Nano Submicron Particle Size and Zeta Potential Particle Analyzer, Delsa™Nano UI Software Versions 2.31/2.03.

### 3.3.7 Basicity

The catalyst basicity was measured by Hammett indicators benzene carboxylic acid titration method [Yan et al., 2009] by using indicators having  $pK_{BH}^+$  in between 6.8-15.0 (Neutral red, Bromothymol blue, Phenolphthalein, Nile blue, Trapeolin and 2,4-dinitroaniline). Sample was placed into a 100 ml flask having a stopper and containing 20 ml of benzene with 1 ml of indicator solution. Then 0.1 N benzoic acid in benzene was added dropwise from micro-burette. End-point was considered at which all the green colour disappeared. Basicity is expressed in terms of mmoles/g and calculated by the titre, 0.1 N of benzoic acid, essential for the amount of solid sample.

### 3.4 Biodiesel production via transesterification reaction and optimization of several reaction parameters

The most frequent method used for biodiesel production is transesterification of the feedstock in presence of alcohol and catalyst. The activities of synthesized catalyst were estimated by trans-esterifying WVO and Karanja oil with methanol in batch type reaction.

Waste vegetable oil (WVO) which was used as one of the feedstock obtained from local restaurant was first filtered to eliminate the suspended matter present in the oil. Then, it was dried in a hot air oven at 110 °C for 2 h to eliminate the moisture content. The acid value of WVO was determined as per ASTM standards and was observed to be

2.36 mg KOH/g. This acid value of WVO is sufficiently low to proceed for direct transesterification.

Karanja oil (*Pongamia pinnata*) used as a feedstock was obtained from local market was dried in a hot air oven for 2 h at 110 °C. The acid value of Karanja oil was determined as per ASTM standards and was observed to be 5.60 mg/KOH, and hence before transesterification reaction; acid esterification was executed to lower its acid value. Acid esterification was performed in 250 ml three neck flask equipped with condenser, mechanical stirrer and thermometer in water bath. Acid esterification was attained by using 1% (v/v) H<sub>2</sub>SO<sub>4</sub> as a catalyst with 1:6 (oil/methanol) molar ratio for 2 h at 60 °C. Stirring was kept constant at 600 rpm to overcome the mass transfer limitations. Reaction mixture was transferred in a separating funnel and water formed with the product was eliminated by decanting. The acid value of esterified oil was found to be 0.52 mg KOH/g and it was within ASTM standards and was used for further transesterification reaction.

The catalysts were found to be more proficient hence utilized for optimization of reaction parameters for enhanced catalytic activity in transesterification reaction. Series of transesterification processes were carried out in order to conclude reaction conditions for optimization purpose by varying parameters. Under the optimization conditions, reusability of catalyst was also estimated. All the transesterification experiments were performed thrice and uncertainties were also studied.

### 3.4.1 Effect of catalyst concentration

In present study, amount of catalyst differed from 1.0 wt% to 5.0 wt% for beta potassium dizirconate, 0.2 wt% to 1.4 wt% for barium zirconate, 0.5 wt% to 3.5 wt% for calcium aluminate and 1.0 wt% to 5.0 wt% for guinea fowl bone derived catalyst were considered. Meanwhile, molar ratio (oil: methanol), reaction temperature and time were

set to their optimum conditions. Moreover, the stirring speed was fixed to optimum speed and FAME conversion was calculated from  $^1\text{H}$  NMR technique.

### 3.4.2 Effect of molar ratio

The effect of oil to methanol molar ratio of beta potassium dizirconate series was varied from 1:4 to 1:12 molar ratio, barium zirconate catalysed series was varied from 1:6 to 1:30 molar ratio, calcium aluminate catalysed series was varied from 1:6 to 1:24 molar ratio and guinea fowl bone derived catalyst series was varied from 1:4 to 1:24 molar ratio. Catalyst concentration, reaction time and temperature were fixed at their optimum conditions. Besides, the stirring speed was also set to optimum and FAME conversion of each set as well as optimum oil: methanol ratio was determined by using  $^1\text{H}$  NMR technique.

### 3.4.3 Effect of reaction temperature

Reaction temperature was varied from 35 °C to 75 °C with interval of 10 °C for each set of experiments however, molar ratio, catalyst concentration, reaction time and stirring speed were kept at their optimum conditions as determined earlier. Then, FAME conversion for various sets was equated and optimum reaction temperature was obtained.

### 3.4.4 Effect of reaction time

Transesterification reaction was carried out at different contact time ranging from 30 min to 150 min for beta potassium dizirconate based transesterification while, 30 min to 210 min for barium zirconate catalysed transesterification whereas, 30 min to 180 min for calcium aluminate catalysed transesterification and 30 min to 210 min for guinea fowl derived catalysed transesterification reaction. FAME conversion was calculated at

optimized reaction condition of catalyst concentration, molar ratio, reaction temperature and stirring speed by  $^1\text{H}$  NMR technique and optimum reaction time was attained.

### 3.4.5 Effect of stirring speed

The influence of stirring speed has been studied in the range of 200 rpm to 700 rpm for beta potassium dizirconate and barium zirconate catalysed reaction whereas 200 rpm to 800 rpm for calcium aluminate and guinea fowl bone derived catalyst system. Molar ratio, catalyst concentration, reaction temperature and time were fixed to optimum conditions. FAME conversion was determined by  $^1\text{H}$  NMR technique.

### 3.4.6 Catalytic activity and reusability

FAME was synthesized in a three neck round bottom flask with reflux system as mentioned as above. Optimum catalyst loading was used at each stage. Catalyst was activated primarily by refluxing it with methanol before addition of feedstock. After every successful run, the catalyst was washed with methanol to purge any kind of organic impurity and then catalyst was dried in a hot air oven for 3-4 h at 120 °C to remove moisture and then was calcined at 600 °C for 2-3h. FAME conversion was estimated in terms of ester content and was analysed by Fourier transform proton-1 nuclear magnetic resonance (FT- $^1\text{H}$  NMR). This process was repeated at each step and hence catalytic activity and reusability has been checked.

## 3.5 Gas chromatography-mass spectrometry (GC-MS) analysis of feedstock

Gas chromatography coupled with mass spectrometry (GC-MS) is used for the investigation of mixture containing unknown organic compounds. GCMS detection has been effectively used to recognize and determine free fatty acid content in order to

produce a unique fingerprint for each feedstock of biodiesel.

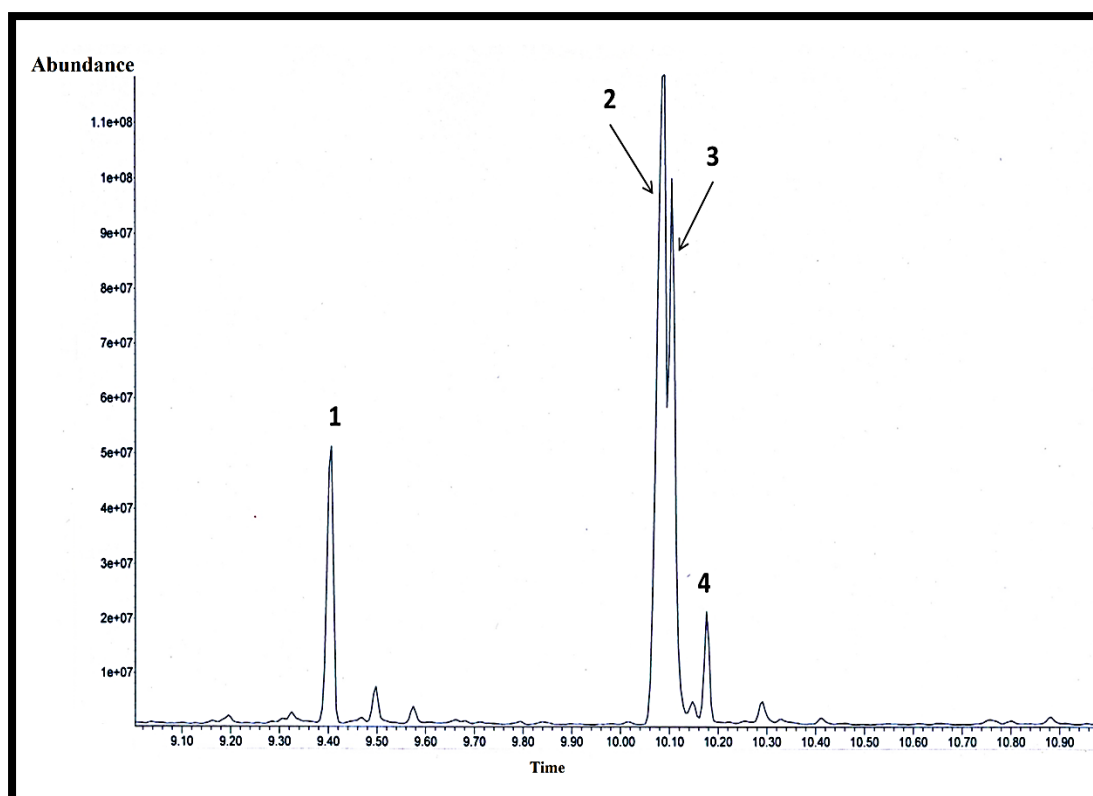
GC-MS of feedstocks were performed on an Agilent Technologies 6890 GC, furnished with mass selective detector (Agilent Technologies) of model 5973. The GC-MS studies were achieved in electron ionization (EI) mode. A DB-5MS (Agilent technologies) capillary column (30 m × 0.25 mm I.D., 0.25 μm film thickness) and helium as carrier gas (constant flow rate of 1.0 mL min<sup>-1</sup>) was used. The GC oven temperature was programmed from 50 °C (2 min) -250 °C at 20 °C min<sup>-1</sup> - 300 °C (3 min) at 50 °C min<sup>-1</sup>. The samples (1 μL) were evaluated in split less mode on an injection temperature of 250 °C. Ionization energy was 70 eV, EI source was set at 230 °C and quadrupole analyser temperature was fixed to 150 °C. Quantitative studies were accomplished in the selected ion monitoring (SIM) mode. Scan range for full scan mode was in between *m/z* 35 to 450 (3.47 scans/second). Data was recorded and compared on the basis of NIST database.

### 3.5.1 Waste vegetable oil (WVO)

GC-MS analysis was conducted to analyse fatty acid composition of WVO. Components existing in sample were recognized, designated and shown in Table 3.1 on the basis of database of NIST. As shown in Table, fatty acid compositions present in WVO were Palmitic acid, Linoleic acid, Oleic acid and Stearic acid at retention time of 9.85, 10.48, 10.49 and 10.57 min respectively. Gas chromatogram of WVO consisting of major components was shown in Figure 3.1. Palmitic acid was 21.46 wt%, Linoleic acid was 38.45 wt%, Oleic acid was 29.12 wt% and Stearic acid was 4.02 wt% with this 6.95 wt% of unidentified component was present in the crude waste vegetable oil.

**Table 3.1** Free fatty acid composition of WVO from GC-MS analysis

Peak	Retention time (min)	Fatty acid composition of oil	Composition (wt%)	Library match
1	9.85	Palmitic acid (C16:0)	21.46	99
2	10.48	Linoleic acid (C18:2)	38.45	99
3	10.49	Oleic acid (C18:1)	29.12	98
4	10.57	Stearic acid (C18:0)	4.02	99
		Unidentified	6.95	

**Figure 3.1** GC-MS chromatogram of waste vegetable oil (WVO)

### 3.5.2 *Pongamia pinnata* (Karanja) oil

GC–MS analysis was accomplished to determine fatty acid composition of Karanja oil. Gas chromatogram of Karanja was shown in Figure 3.2. Mass spectrum interpretation was carried by means of database of NIST. The fatty acid compositions present in the sample were identified and described in Table 3.2. As shown in chromatogram, the major components present were Palmitic acid, Linoleic acid, Oleic acid, Stearic acid, Vaccenic acid, Stearic acid, Lignoceric acid and Oleic acid at retention time of 10.84, 11.10, 11.13, 11.22, 11.56, 11.65, 13.28, 13.32 min respectively. Palmitic acid was 12.67 wt%, Linoleic acid was 3.46 wt%, Oleic acid was 32.36 wt%, Stearic acid was 1.11 wt%, Vaccenic acid was 42.47 wt%, Stearic acid was 2.11 wt%, Lignoceric acid was 1.50 wt% and Oleic acid was 2.31 wt% with this 2.01 wt% of unidentified component were present in the crude Karanja oil.

**Table 3.2** Free fatty acid composition of Karanja oil from GC-MS analysis

Peak	Retention time (min)	Fatty acid composition of oil	Composition (wt%)	Library Match
1	10.84	Palmitic acid (C16:0)	12.67	99
2	11.10	Linoleic acid (C18:2)	3.46	99
3	11.13	Oleic acid (C18:1)	32.36	99
4	11.22	Stearic acid (C18:0)	1.11	98
5	11.56	Vaccenic acid (C18:1)	42.47	95
6	11.65	Stearic acid (C18:0)	2.11	98
7	13.28	Lignoceric acid (C24:0)	1.50	94
8	13.32	Oleic acid (C18:1)	2.31	95
		Unidentified	2.01	

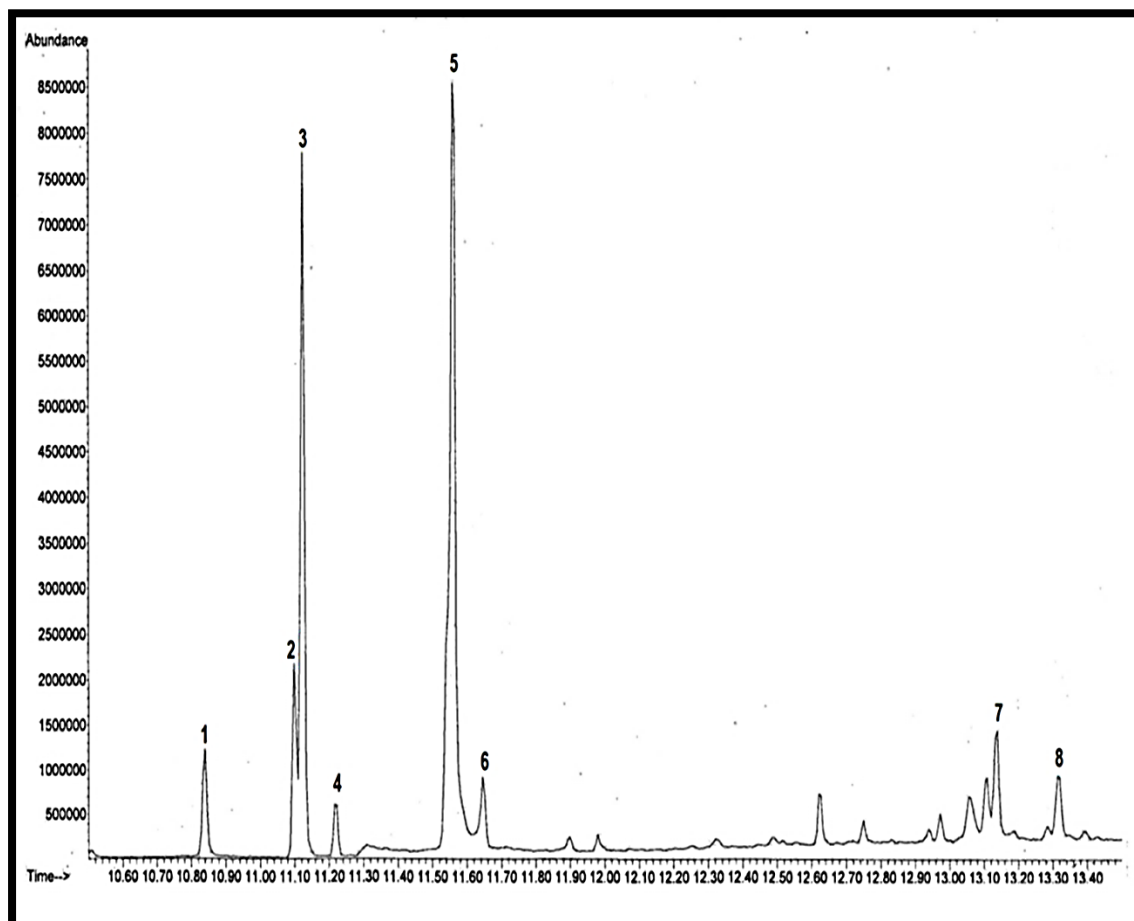


Figure 3.2 GC-MS chromatogram of Karanja oil

### 3.6 Fourier transform proton-1 nuclear magnetic resonance (FT- $^1\text{H}$ NMR) of product (biodiesel)

The percentage conversions of triglyceride to methyl ester were quantified by  $^1\text{H}$  NMR technique as reported in literature [Knothe, 2001]. Fourier transform-proton 1 nuclear magnetic resonance (FT- $^1\text{H}$  NMR) spectra of synthesized FAME were recorded on BRUKER 500 Ascend<sup>TM</sup> 500 (advance III HD) instrument by using  $\text{CDCl}_3$  as a solvent and TMS as internal reference. Fatty acid methyl ester content in percent was calculated by using Equation 3.1 [Knothe, 2001].



$$\text{FAME conversion (\%)} = (2 A_{\text{ME}}/3 A_{\alpha\text{CH}_2}) * 100 \quad \dots(\text{Equation 3.1})$$

Where,  $A_{\text{ME}}$  represents the integration value of methyl ester proton (strong singlet) and  $A_{\alpha\text{CH}_2}$  shows the integration value of methylene proton. The factors 2 and 3 are resultant of the fact that the methylene carbon has two protons, whereas methoxy derived carbon possesses three attached protons.

### 3.7 American Society for Testing and Materials (ASTM) specifications

The characteristics of feedstock and biodiesel were determined as per American Society for Testing and Materials (ASTM). As standardization is a criterion for prosperous market introduction and dissemination of biodiesel, standards for biodiesel quality has been defined in various countries. Quality of biodiesel has been defined by various parameters such as acid value, density, cetane number, kinematic viscosity, calorific value, flash point, fire point, cloud point, pour point and ash content have been investigated as per ASTM D6751 [Tariq et al., 2011] standards. Table 3.3 shows the ASTM test methods used to study properties of fuel as well as the limit of standard biodiesel in comparison to neat diesel fuel.

#### 3.7.1 Acid value

Acid value or acid number is the measure of content of free fatty acid present in the oil sample. Acid value defined as number of milligram of KOH required for neutralizing free fatty acids present in 1 g of oil or fat. Acid value has determined as per ASTM D664 standards. If acid value is more than 4, then it requires acid esterification before transesterification reaction to lower its acid value, otherwise saponification will occur.

**Table 3.3** ASTM specifications of biodiesel and diesel fuel

Parameters	ASTM test Method used	ASTM-6751 Biodiesel	Diesel fuel
Acid value (mg KOH/g)	D664-07	< 0.8	0.36
Density (40 °C, g cm <sup>-3</sup> )	D1448-1972	0.86-0.90	0.840
Kinematic viscosity (cSt at 40 °C)	D445	1.9-6.0	2.98
Cetane number	D613	47 min	40
Calorific value (MJ/Kg)	D6751/ DIN51900	35 min	44
Flash point (°C)	D93	100-170	52
Fire point (°C)	D93	-	89
Cloud point (°C)	D2500	-3 to 12	-
Pour point (°C)	D97-05	-15 to 16	-
Ash content (%)	D482	< 0.02	0.01

### 3.7.2 Density

Biodiesel is denser than conventional diesel fuel and this consents application of splash blending by addition of biodiesel on the top of diesel for making of biodiesel blends. Density has been derived as per ASTM D1448-1972 standards.

### 3.7.3 Kinematic viscosity

Kinematic viscosity is an essential characteristic of biodiesel since it disturbs fuel injection equipment's operation. It measures the resistance to flow due to internal friction and is determined by capillary viscometer as per ASTM D445 test method. Greater kinematic viscosity shows poor atomization of fuel, carbon deposition on injector as well as incomplete combustion. Viscosity is directly commensurable to density and by

performing simply transesterification reaction viscosity of oil can be decreased.

### **3.7.4 Cetane number**

Cetane number plays an important role for fuel quality and correlates with the combustion quality and ignition delay time; hence a competent cetane number is obligatory for good engine performance. Higher cetane number shows improved ignition properties. Biodiesel shows higher cetane number as compared to diesel fuel which results into higher combustion efficiency with smoother combustion. Cetane number of the biodiesel has been determined as per ASTM D613 test method.

### **3.7.5 Calorific value**

Calorific or heating value is the extent of heat released through complete combustion of fuel. ASTM D6751 test method has been referred for calorific value measurement. Biodiesel possesses lower calorific value in comparison to diesel fuel due to presence of excessive oxygen content.

### **3.7.6 Flash point and fire point**

Flash point of the fuel is minimum temperature at which fuel will ignite when exposed to an ignition source. Fire point is the temperature at which fuel vapour will burn continuously after ignition for minimum 5 seconds in open flame. Flash point and fire point have been determined as per ASTM D93 standards. Proper handling and safety is required for fuel having low flash point. Flash point of biodiesel is greater as compared to petro diesel; hence it is safe for transportation as well as reduces the risk of fire.

### 3.7.7 Cloud point and pour point

Cloud point and pour point have been determined as per ASTM D2500 and ASTM D97-05 test methods, respectively. Cloud point is the temperature at which fuel shows a haze of wax (cloud) when cooled at standard test conditions. Whereas, pour point is the temperature at which fuel will just flow at standard conditions.

### 3.7.8 Ash content

Ash content measures the amount of inorganic matter which is non-combustible in nature. ASTM D482 test methods have been used to determine the ash content in fuel. High ash content causes wear of injection system, injector tip plugging as well as deposition during combustion. Lesser ash content promotes longer value life of engine.